Theoretical and experimental research on cryogenic Yb:YAG regenerative amplifier

Xinghua Lu (卢兴华)*, Jiangfeng Wang (王江峰), Xiang Li (李　响), Youen Jiang (姜有恩), Wei Fan (范　薇), and Xuechun Li (李学春)

Shanghai Institute of Optics and Fine Mechanics, Chinese Academy of Sciences, Shanghai 201800, China

**Corresponding author: luxingh@yahoo.cn*

Received April 14, 2011; accepted May 9, 2011; posted online July 11, 2011

Based on the theory of quasi-three-level rate equations modified by amplified spontaneous emission, the stored energy density and the small signal gain of the cryogenic Yb:YAG regenerative amplifier for a given geometry for pulsed pumping in three dimensions are theoretically studied using the Monte Carlo simulation. The present model provides a straightforward procedure to design the Yb:YAG parameters and the optical coupling system for optimization when running at cryogenic temperature. A fiber-coupled laser diode end-pumped cryogenic Yb:YAG regenerative amplifier running at 1 030 nm is demonstrated with a maximum output energy 10.2 mJ at a repetition rate of 10 Hz. A very good agreement between the experiments and the theoretical model is achieved.

OCIS codes: 140.3430, 140.3280, 140.3580.

doi: 10.3788/COL201109.111401.

With the development of high power laser diodes (LDs), rare earth ion-doped materials have attracted great interest in the application of high-efficiency and high-power diode pumped laser systems[1,2]. Among these laser ions, trivalent ytterbium (Yb) seems to be the most appealing because of its simple electronic structure[3]. Its electronic level diagram consists of only two electronic levels, avoiding the excited state absorption, up conversion processes, and concentration quenching. Yttrium aluminum garnet (YAG) is an attractive laser host material because of its excellent thermal, chemical, and mechanical properties[4]. Compared with Nd:YAG laser crystals, Yb:YAG has several advantages, such as a long fluorescence lifetime and a very low quantum defect, resulting in three times less heat generation during lasing than Nd-based laser systems. The longer fluorescence lifetime benefits energy storage. The lower quantum defect of Yb causes less heat deposition, enabling the operation of the laser at higher repetition rates. Other advantages include broad absorption bandwidth and less sensitivity to diode wavelength specifications, a relatively large emission peak cross-section, and easy growth with high quality and high doping concentration[5]. Several types of Yb:YAG lasers have been developed for efficient oscillation with various pumped architectures, including thin disk[6], microchip[7], and rod[8] structures at room temperature. The primary disadvantage of Yb lies in its quasi-three-level nature. Therefore, high pump fluence is required to overcome the re-absorption losses and to reach high storage efficiency at room temperature. The quasi-three-level nature of this material can be overcome by using the material under cryogenic cooling condition. The benefits of cooling Yb:YAG result in a significant increase in the emission cross section; the thermal properties of Yb:YAG, such as thermal conductivity, thermo-optic coefficient, and thermal expansion coefficient, are significantly improved at low temperatures, which are preferred especially for high-average-power operation[9].

Considering the increasing emission cross section and the improving thermal behavior of the cryogenic Yb:YAG, high-energy, close to 10-Hz repeatable, nanosecond laser systems have been widely used in various kinds of fields, such as inertial fusion energy and pumped sources for optical parametric amplifiers[10]. Cao *et al.* theoretically researched the efficiency of diode-pumped Yb:YAG disk amplifiers at room temperature[11]. Albach *et al.* numerically simulated the effect of amplified spontaneous emission (ASE) on Yb:YAG slabs in monochromatic assumption[12]. In the current work, a theoretical model based on quasi-three-level rate equations is modified to investigate the cryogenic Yb:YAG regenerative amplifier to obtain the stored energy and the small signal gain coefficient in the crystal by considering the pump pulse duration and length of the crystal. Considering the ASE effect, a number of Monte Carlo simulations, which can estimate the stored energy density for a given geometry for pulsed pumping in three dimensions, are developed. The present model provides a straightforward procedure to design the crystal parameters and the optical coupling system for optimization. To illustrate the utility of the present model, a cryogenic Yb:YAG regenerative amplifier pumped by fiber-coupled LDs is demonstrated. The output beam has a nearly TEM_{00} mode profile with maximum energy obtained at 10.2 mJ at a repetition rate of 10 Hz. A very good agreement between experiments and the theoretical model is observed.

An energy-level diagram of the Yb:YAG is shown in Fig. 1. It consists of only two manifolds, an upper $^2F_{5/2}$ and a lower $^2F_{7/2}$, with the former containing three Stark levels and the latter four[13]. The Boltzmann occupation factors for the upper state manifold are labeled f_{11}, f_{12}, and f_{13}, whereas those for the lower state manifold are labeled f_{01}, f_{02}, f_{03}, and f_{04}. Pumping and lasing processes occur between the Stark sub-levels. Rapid thermalization of the levels within each manifold is assumed so that the relative populations of the levels within a manifold can be treated by the Boltzmann equilibrium[11].

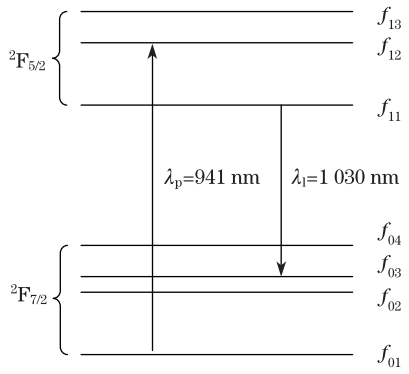

Fig. 1. Energy levels and occupation factors for Yb:YAG.

When the pump radiation is in the form of rectangular pulses of intensity $I^{\rm p}$, the duration t_0 incident (along the z axis) on the active elements' end face with thickness l, concentration of activator ions N_0, upper-level density normalized to the activator ions concentration $x_{\rm u}$, and pump intensity normalized to the saturation pump intensity $I_{\rm p}$ are given by[14]

$$\tau\frac{\partial x_{\rm u}(t,z)}{\partial t}=I_{\rm p}(t,z)[f_{\rm p}-x_{\rm u}(t,z)]-x_{\rm u}(t,z), \quad (1)$$

$$\frac{\partial I_{\rm p}(t,z)}{\partial z}=-\sigma_{\rm p}N_0(f_{01}+f_{12})[f_{\rm p}-x_{\rm u}(t,z)]I_{\rm p}(t,z), \quad (2)$$

$$x_{\rm u}=N_{\rm U}/N_0, \quad (3)$$

$$f_{\rm p}=I^{\rm p}/I_{\rm ps}, \quad (4)$$

where $N_{\rm U}$ is the upper-level population, τ is the upper-state lifetime, $I_{\rm ps}$ is the pump saturation intensity, $\sigma_{\rm p}$ is the absorption cross section, and $f_{\rm p}$ is given by

$$f_{\rm p}=f_{01}/(f_{01}+f_{12}). \quad (5)$$

When the ASE is considered[12], the normalized upper-level density is given as

$$\tau\frac{\partial x_{\rm u}(t,x,y,z)}{\partial t}=I_{\rm p}(t,x,y,z)[f_{\rm p}-x_{\rm u}(t,x,y,z)]-x_{\rm u}(t,x,y,z)M_{\rm ASE}, \quad (6)$$

$$M_{\rm ASE}(x,y,z)=1+\tau\int_{\lambda}[\sigma_{\rm a}(\lambda,x,y,z)[1-x_{\rm u}(x,y,z)]+\sigma_{\rm e}(\lambda,x,y,z)]\phi_{\rm ASE}(\lambda,x,y,z){\rm d}\lambda, \quad (7)$$

$$\phi_{\rm ASE}(\lambda,x,y,z)=\Big\{\int_{V}x_{\rm u}(x',y',z')g(\lambda)G_{(x',y',z')\to(x,y,z)}/\left|\rho[(x',y',z'),(x,y,z)]\right|^2{\rm d}V\Big\}/(4\pi\tau), \quad (8)$$

where the absorption and emission cross sections of spontaneous emission at wavelength λ are $\sigma_{\rm a}$ and $\sigma_{\rm e}$, respectively, ρ is the distance between (x',y',z') and the observed point (x,y,z), $g(\lambda)$ is the line shape function, and $G_{(x',y',z')\to(x,y,z)}$ is the gain.

When the ASE is considered, the Monte Carlo algorithm is required to estimate the stored energy density for a given geometry for pulsed pumping in three dimensions[15]. Using the Monte Carlo approach, five random numbers determine the position (x,y,z) and direction (θ,φ) of the spontaneously emitted beam in each time interval. The spectral distribution of these photons is determined by the specific amplifier medium. The trajectory of this beam is calculated, assuming that the edges of the crystal are totally absorbing. Photons reaching the face with high-reflection coated at 1 030 nm are totally reflected back into the crystal. Photons reaching the face with antireflection coated at 1 030 nm are reflected back into the crystal if $\vartheta>\vartheta_c=\sin^{-1}(1/n)$, where n is the index of refraction of the crystal; otherwise, they exit the crystal. The next beam of photons, emitted from a new random site in a random direction, exhibits lower inversion where the first beam traveled.

At the moment of the pump pulse termination, an amplified laser pulse passes through the crystal. The rate equations governing the amplified process are given by[14]

$$\tau\frac{\partial x_{\rm u}(t,z)}{\partial t}=-I_{\rm l}[x_{\rm u}(t,z)-f_{\rm l}], \quad (9)$$

$$\frac{\partial I_{\rm l}(t,z)}{\partial z}=\sigma_{\rm l}N_0(f_{03}+f_{11})[x_{\rm u}(t,z)-f_{\rm l}]I_{\rm l}(t,z), \quad (10)$$

where $I_{\rm l}$ is the laser intensity normalized to the laser saturation intensity, $\sigma_{\rm l}$ is the emission cross section, and $f_{\rm l}$ is given by

$$f_{\rm l}=f_{03}/(f_{03}+f_{11}). \quad (11)$$

The numerical simulations are computed using this model. Table 1 gives the parameters used in the numerical simulations. Figure 2 shows the time evolution of the stored energy in the presence and absence of ASE. The laser crystal is doped with 8 at.-% Yb ions with a length of 1.8 mm. The spatial profile of the pump beam on the laser crystal is assumed nearly a flat top. At the beginning of the pump process, the ASE can be ignored because of the small upper-level population. The upper-state population density is obviously depleted by spontaneous emission with the increase in the upper-level population. The optimum pump pulse duration is approximately two times of the upper-level lifetime in the case of our pump conditions. In the following numerical calculation, the pump pulse duration is 1.8 ms.

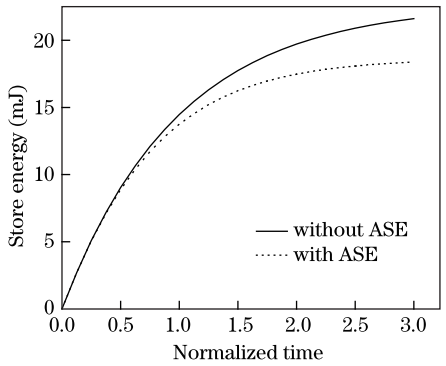

Fig. 2. Store energy versus normalized time (pump pulse duration/upper-state lifetime) with or without ASE.

Table 1. Parameters Used in the Numerical Simulations

Parameter	Value
Temperature (K)	183
Repetition (Hz)	10
Pump Wavelength (nm)	941
Laser Wavelength (nm)	1 030
Pump Absorption Cross Section (cm^2)	1.24×10^{-20}
Laser Emission Cross Section (cm^2)	5.5×10^{-20}
Pump Saturation Intensity (kW/cm^2)	16.8
Laser Saturation Intensity (kW/cm^2)	4.17
Laser Pulse Duration (ns)	10
Upper-State Lifetime (ms)	0.951

For a specific pumping condition and fixed doping density, a maximum thickness of the gain medium accompanying the maximum absorption efficiency exists[11]. If the thickness is too thin, then the pump radiation has inefficient absorption; otherwise, there is efficient absorption but there exist sections of the gain medium not pumped completely enough to reach population inversion. Figure 3 gives the small signal gain coefficient versus the length of the crystal in the absence of ASE. In the case of our pump conditions, the maximum thickness transparent to the amplified laser is 2.3 mm. However, in practice, the maximum thickness is slightly thinner than this value because the presence of ASE considerably depletes the upper-level population. The length of the crystal used in the experiments is 1.8 mm.

Based on the above analysis, a regenerative amplifier with a liquid nitrogen-cooled Yb:YAG crystal is demonstrated. A schematic diagram of the regenerative amplifier is shown in Fig. 4. In this arrangement, the seed source is a continuous wave (CW) distributed feedback fiber laser after an acoustic-optic chopper and optical fiber amplifiers, which produce 10-ns pulses with a 10-Hz repetition rate at a wavelength of about 1 030 nm. The crystal has one side high-transmission coated at 941 nm and high-reflection coated at 1 030 nm, and another side that is antireflection coated at 1 030 nm. The crystal mounted on the copper heat sinks at 183 K is attached to a liquid nitrogen cryostat in vacuum. The heat sinks have liquid nitrogen flowing through them via hoses connected to a liquid nitrogen reservoir. The crystal is uniformly cooled through the transverse surface, which is in contact with the heat sinks cooled by liquid nitrogen to remove the heat generated in the crystal. This open cycle cooling approach vents gas to the atmosphere after the cryogen passes through the heat sinks, removing heat from the crystal. An indium foil placed between the crystal side faces and the heat sinks provides efficient thermal contact.

The pump energy from a LD is coupled into the fiber and then strongly focused by lens into the gain medium. The pump duration is 1.8 ms, and the repetition rate is 10 Hz with a maximum pump power of 120 W. The spatial profile of the pump beam on the laser crystal is presented in Fig. 5.

A combination of a thin-film polarizer, a quarter-wave plate, and a Pockels cell is used for the injection and extraction of the laser pulses in the cavity of the regenerative amplifier. An operational cycle of the regenerative amplifier consists of two successive stages. When voltage is not applied to the Pockels cell, the quarter-wave plate, along with the polarizer, provides high intracavity losses. Laser action is suppressed by high losses, and the gain medium, which is under continuous pumping, accumulates population inversion. The amplification takes place when quarter-wave voltage is applied to the Pockels cell, and the seed pulse is injected into the resonator. The intracavity pulse energy grows until the gain becomes equal to the resonator losses. The Pockels cell voltage is then switched off, dumping the amplified pulse out of

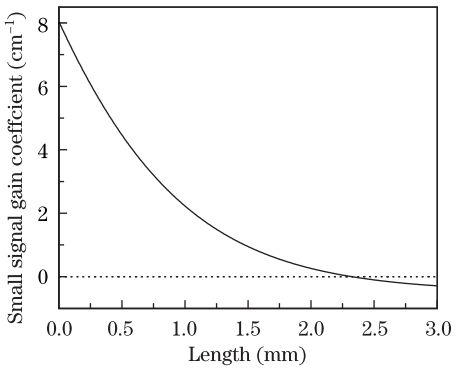

Fig. 3. Small signal gain coefficient versus length of the crystal.

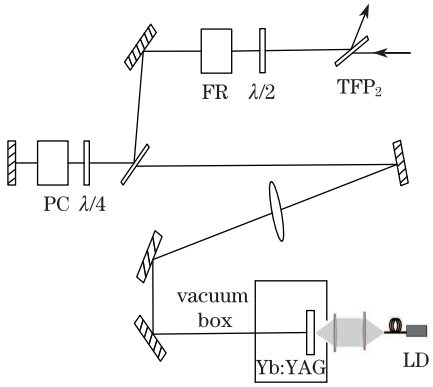

Fig. 4. Schematic of the regenerative amplifier with a liquid nitrogen-cooled Yb:YAG crystal. TFP: thin-film polarizer; $\lambda/2$: half-wave plate; $\lambda/4$: quarter-wave plate; PC: Pockels cell; FR: Faraday rotator.

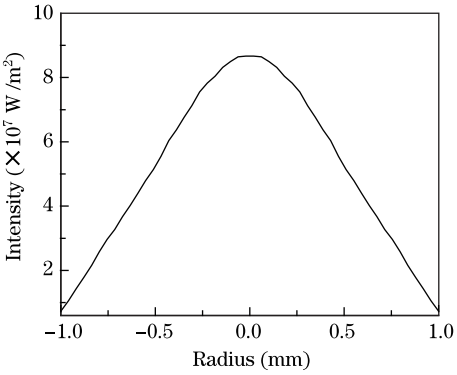

Fig. 5. Spatial profile of the pump beam.

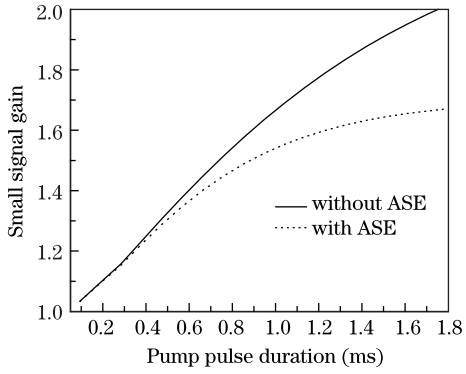

Fig. 6. Small signal gain versus pump pulse duration.

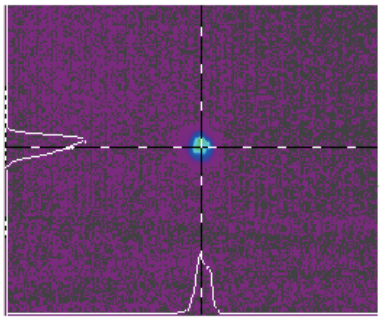

Fig. 7. Mode profile of the output beam.

the cavity as the output pulse.

Figure 6 shows the small signal gain versus the pump pulse duration. The small signal gain measured in the experiments is 1.70, which agrees well with the results of the theoretical calculations. It is about 1.67, as presented in Fig. 6. The reason why the theoretical value is slightly smaller is because a limited width of the fluorescence in the Monte Carlo simulation is required to speed up the calculation. If the ASE effect is not considered, the numerically obtained small signal gain of about 2.0 has an obvious deviation compared with the practical situation. The larger the gain of the medium, the more spontaneous emission is amplified, which results in the reduction of the expected inversion calculated in the absence of ASE. Thus, increasing the gain results in increased ASE, which decreases the inversion and gain. In turn, this decrease leads to the limiting of the gain, which can be achieved from an amplifier by increasing its size, pumping rate, or doping. ASE becomes the dominant decay mechanism in the regenerative amplifier.

The maximum energy obtained in the experiment is 10.2 mJ, with a 10-Hz repetition rate. Figure 7 shows the measured mode profile of the output beam. The laser output beam has a nearly TEM_{00} mode profile in both directions, with $M_x^2 = 1.24$ and $M_y^2 = 1.18$ in the horizontal and vertical planes, respectively. The slightly elliptical laser output beam may be caused by the thermal effects. Thermal lensing and the resulting phase distortions in the gain medium influence the output stability of the regenerative amplifier. In addition, the thermally induced birefringence in the gain medium, which can perturb the linear polarization of the laser pulse, induces additional losses at the polarizer. The thermal effects, which are a severe limitation in scaling the output power of the regenerative amplifier, deserve further research.

In conclusion, the characteristics of the cryogenic Yb:YAG regenerative amplifier are numerically researched based on quasi-three-level rate equations in the presence of ASE. A fiber-coupled LD end-pumped cryogenic Yb:YAG regenerative amplifier running at 1 030 nm is demonstrated with maximum output energy 10.2 mJ at a repetition rate of 10 Hz. The experimental data measured in the cryogenic Yb:YAG regenerative amplifier are in accordance with the theoretical results.

References

1. J. He, X. Liang, L. Zheng, L. Su, J. Xu, and Z. Xu, Chin. Opt. Lett. **7,** 1028 (2009).
2. Y. Lü, J. Xia, J. Wang, A. Zhang, X. Zhang, L. Bao, H. Quan, and X. Yin, Chin. Opt. Lett. **8,** 187 (2010).
3. W. F. Krupke, IEEE J. Sel. Top. Quant. Electron. **6,** 1287 (2000).
4. T. Fan and J. Daneu, Appl. Opt. **37,** 1635 (1998).
5. J. Dong, A. Shirakawa, K. I. Ueda, and A. A. Kaminskii, Appl. Phys. B: Lasers and Optics **89,** 367 (2007).
6. E. Innerhofer, T. Südmeyer, F. Brunner, R. Häring, A. Aschwanden, R. Paschotta, C. Hönninger, M. Kumkar, and U. Keller, Opt. Lett. **28,** 367 (2003).
7. J. Dong, A. Shirakawa, K. I. Ueda, and A. A. Kaminskii, Appl. Phys. B: Lasers and Optics **89,** 359 (2007).
8. S. Wang, J. Chen, C. Liu, M. Hu, J. Ge, G. Zhao, and J. Xu. Chinese J. Lasers (in Chinese) **36,** 23 (2009).
9. D. C. Brown, IEEE J. Sel. Top. Quant. Electron. **11,** 587 (2005).
10. J. Kawanaka, N. Miyanaga, T. Kawashima, K. Tsubakimoto, Y. Fujimoto, H. Kubomura, S. Matsuoka, T. Ikegawa, Y. Suzuki, N. Tsuchiya, T. Jitsuno, H. Furukawa, T. Kanabe, H. Fujita, K. Yoshida, H. Nakano, J. Nishimae, M. Nakatsuka, K. Ueda, and K. Tomabechi, Journal of Physics: Conference Series. **112,** 032058 (2008).
11. D. Cao, H. Yu, W. Zheng, and S. He, Proc. SPIE **6823,** 682309 (2007).
12. D. Albach, J.-C. Chanteloup, and G. le. Touzé, Opt. Express **17,** 3792 (2009).
13. D. C. Brown and V. A. Vitali, IEEE J. Quantum Electron. **47,** 3 (2011).
14. G. L. Bourdet, Opt. Commun. **200,** 331 (2001).
15. C. Goren, Y. Tzuk, G. Marcus, and S. Pearl, IEEE J. Quantum Electron. **42,** 1239 (2006).